

Anticipation decides on lane formation in pedestrian counterflow – a simulation study

Emilio N.M. Cirillo

E-mail: emilio.cirillo@uniroma1.it

Dipartimento di Scienze di Base e Applicate per l'Ingegneria, Sapienza Università di Roma, via A. Scarpa 16, I-00161, Roma, Italy.

Adrian Muntean

E-mail: adrian.muntean@kau.se

Department of Mathematics and Computer Science, Karlstad University, Sweden.

Abstract. Human crowds base most of their behavioral decisions upon anticipated states of their walking environment. We explore a minimal version of a lattice model to study lanes formation in pedestrian counterflow. Using the concept of horizon depth, our simulation results suggest that the anticipation effect together with the presence of a small background noise play an important role in promoting collective behaviors in a counterflow setup. These ingredients facilitate the formation of seemingly stable lanes and ensure the ergodicity of the system.

Keywords: Stochastic dynamics, lane formation, anticipation.

Appunti: November 23, 2021

1. Introduction

1.1. Lanes in counterflow

Very much like colloids or bacteria colonies, human crowds can be thought of as many-particle interacting systems. From this perspective, the non-equilibrium statistical mechanics becomes the right language to study large crowds coming into play, where highly complex situations giving rise to interesting collective phenomena, such as free flow, lanes¹, and gridlock or jamming (cf. [3, 10, 24, 22], e.g.), may arise.

This paper focuses on *lane formation* in pedestrian counterflow, i.e., a bidirectional pedestrian movement. The novelty we bring into this context is linked to the ambition to reproduce

¹One of the most efficient transport mechanisms in crowded situations – like those where active colloidal particles are supposed to cross soft matter solutions – or when pedestrian counterflow in Tokyo's Shibuya and Shinjuku railways stations thrives for fluidization – are lanes. An average of 3.5 million people per day use the Shinjuku station, making it the busiest station in the world in terms of passenger numbers. Shibuya station is similarly busy.

the rational behaviour of individuals forming lanes through the means of anticipation, an old idea that can be traced back at least from Oresme’s time; see [21]. From this perspective, we are in line with some of the statements in [2] and complement existing research on the lane formation topic in pedestrian counterflows.

1.2. A brief literature review on lane formation

The mechanisms yielding lane formation are still obscure and object of current research from both theoretical and experimental viewpoints. From the crowd management perspectives, one strongly believes that controlling in real time the building up and the dissolution of lanes would be an efficient tool both for organization matters as well as for what concerns the activity of responsible law enforcement agencies. Regarding lane formation, we refer the reader to [19] for a review from the point of view of self-organization, to [17] for a perspective from the transportation engineering side, as well as to own previous research [11] where we attempted to investigate pedestrian counterflows through heterogeneous domains. Lane formation has been observed in many empirical studies (see the discussion in [14, Section 4.1]) and it has also been noted that a certain degree of noise favors lane formation, whereas a too large noise amplitude lead to a “freezing by heating” effect [15, 16]. It is worth also looking into the recent study [18], where lanes are perceived as super-diffusive Lévy walks. The formation of lanes has been quite well described in the framework of the *social force model* [13, 14], whereas it has been considered a quite hard phenomenon to be described in the framework of more elementary *cellular automata* models [7, 8]. Related ideas are reported, for instance, also in [1, 9]. The main drawback of the social force model is that it involves a large number of parameters. An important breakthrough in this direction can be considered the paper [4] in which the idea of the *floor field* cellular automaton has been firstly introduced. In this model the floor field is constructed dynamically during the evolution of the system and allows the coupling between the motion of the particles and a sort of *trace* left by particles which moved before [19, 23]. The floor field is traditionally made of a *static* and a *dynamic* component [4]. More recently a so called *anticipation* component has also been taken into account [19, 23]. We refer the reader to [12] for an account of anticipation effects in the context of deterministic dynamical system modeling pedestrian motion. The static floor field is constant in time and not influenced by the presence of other particles, it simply codes the preferential direction of motion of each particle. The dynamic floor field, inspired by the motion of ants who leave pheromone traces which can be smelled by other ants, evolve with time and codes the trace left by moving pedestrians. The anticipation floor field allows pedestrian to estimate the route of pedestrians moving in the opposite direction and try to avoid collisions.

1.3. Aim of this research

In this framework, we propose an elementary model as well as a different mechanism for lane formation. The main idea behind this mechanism is mildly related to the anticipation floor field just discussed previously. The aim of our study is to bring evidence that the elementary mechanism yielding lane formation is the pedestrian’s attitude to avoid collisions with pedestrians moving in the opposite direction, i.e. the *anticipation*.

To keep as simple as possible the modeling level, we use a lattice model approach. We define a discrete time dynamics on a lattice with an exclusion rule, namely, each site can be occupied by a single particle at time. The formation of lanes at stationarity is studied by means of the order parameter proposed in [19]. We demonstrate that, provided the attitude to avoid collisions is relevant enough, lanes naturally appear in the system. This is in our view the main mechanism leading to the formation of lanes.

The rest of the paper is organized as follows. In Section 2.1 we describe in more detail the crowd dynamics scenarion we have in mind. The model is presented in Section 2.2. The results of our simulations are discussed in Section 3, whereas our conclusions are finally summarized in Section 4.

2. The model

In this section, we present the crowd dynamics scenario we have in mind. Here we define the chosen modeling strategy and briefly explain the main observables that will be closely followed in our simulations. These observables are our main tools to explore the internal coherent crowd structures which are expected to form in pedestrian counterflows.

2.1. Pedestrian counterflow as a Gedankenexperiment

Our crowd dynamics setup is as follows: Two different types of pedestrians enter a vertical strip: those moving upward (“red particles”) and those moving downward (“blue particles”). At each time the pedestrians move mostly forward with respect to their preferential direction, but they will have a small probability r , called the *background noise*, to do something different, namely, stepping laterally or even moving backward. This noise mimics the presence of irregularities (small obstacles) in the strip, or simply, the pedestrian’s loss of visual focus due to interactions with the surrounding ambient as it is often promoted in environmental psychology reports. The reason for such a background noise is also technical. Indeed, the mathematical model turns to be a discrete time Markov Chain. In the case $r = 0$, the model would exhibit many absorbing varieties made of those configurations in which particles are perfectly in-lane. In other words, set of configurations in which columns are occupied either

by red or blue particles would be absorbing varieties of the state space. Considering $r > 0$ simply ensures the ergodicity² of the model.

Pedestrians do not move simultaneously, but sequentially; namely, the new position reached by a particular pedestrian has to be taken into account when moving the following one. For this reason, we refer to our model as *lattice model* rather than cellular automaton.

The distinguishing feature we introduce in this context is the idea of *horizon*: if one pedestrian spots another one moving in the opposite direction in front of him within an *a priori* fixed distance (i.e., the horizon depth), then she/he will try to step laterally with the probability h . The correlation between the lateral motion of a particle and the approaching of an opposing one will yield lane formation as we see in Section 3. The model will be explored by numerical simulations for different values of the parameters. Having in view the application to pedestrian motions, the relevant parameter regime is $r \ll 1$ (low noise background) and $h \gg 0$ (large avoiding tendency).

2.2. Definition of the model

The model is very much inspired by the one proposed by the authors in [5, 6]. The walking space is chosen to be the *strip* $\Lambda = \{1, \dots, L_1\} \times \{1, \dots, L_2\} \subset \mathbb{Z}^2$. Each *site* or *cell* in Λ can be either empty or occupied by a single particle (hard core repulsion).

Each particle is either *red* or *blue*. For red particles, the *forward* direction is downward, whereas for blue particles the forward direction is upward. We let N_r and N_b be the number of red and blue particles at the initial time $t = 0$, respectively. We let $N := N_r + N_b$ be total number of particles at the initial time and $n(t)$ be the total number of particles at time t .

Particles are labelled. At each step of the dynamics, we choose sequentially at random with uniform probability one of the N particles. If the particle lies in the lattice, then we displace it with the probabilities specified below: if the cell where the particle should be moved to is occupied, then the particle is not moved (hard core repulsion acts accordingly to the simple exclusion rule). Time is increased by one after N particles have been selected and possibly moved.

We let $r \in [0, 1]$ be the *background noise* and $h \in [0, 1]$ be the *lateral move probability*. Moreover, given a particle, its *horizon* is the vertical slab made of the first $H \geq 0$ cells (up or down to the last cell of the strip) the selected particle would visit during its forward motion. The integer number H will be called *horizon depth*.

Either a red particle moves to one of the four neighboring cells with probabilities $1 - 3r/4$ (down), $r/4$ (left), $r/4$ (right), and $r/4$ (up) if $H = 0$, or the horizon is empty, or the closest particle in the horizon is red. Otherwise, it moves to one of the four neighboring cells with

²Ergodicity is lost for instance when an horizontal line with blue particles opposing red particles is formed.

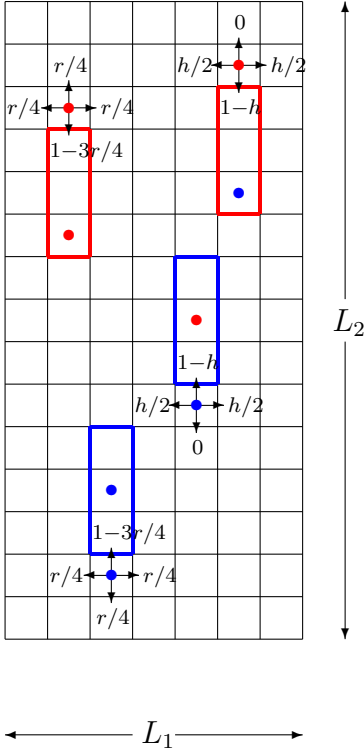


Figure 1: Schematic representation of the model for horizon $H = 3$. Arrows denote possible moves and the related probabilities are reported in the cell.

probabilities $1 - h$ (down), $h/2$ (left), $h/2$ (right), and 0 (up), see Figure 1.

Similarly, either a blue particle moves to one of the four neighboring cells with probabilities $1 - 3r/4$ (up), $r/4$ (left), $r/4$ (right), and $r/4$ (down) if $H = 0$, or the horizon is empty, or the closest particle in the horizon is blue. Otherwise, the particle moves to one of the four neighboring cells with probabilities $1 - h$ (up), $h/2$ (left), $h/2$ (right), and 0 (down).

The fact that the jumping probabilities change when an opposing particle is spotted inside the horizon will be addressed as *anticipation mechanism*. The parameter r is called background noise. The model aims to describe two families of pedestrians one heading down and the other heading up. This is precisely what happens in our model with the red and blue particles if $r = 0$. However, when r is positive, different moves are allowed in the system as it happens to real pedestrian crowds in motion – sometimes they displace not following their prescribed best trajectory, but with random shifts due to external noise, such as sounds, light flashes, images, or obstacles. Note that if r is small, red and blue particles experience an important downward and, respectively, an upward drift, which becomes smaller when r

increases and finally disappears at $r = 1$, when the walk becomes perfectly symmetric.

We introduced the parameter r not only to mimic random real world shifts, but also for a technical reason. Indeed, in the case $H = 0$, namely, when the anticipation effect is not considered, for $r = 0$ our model would be completely trivial, indeed, red and blue particles would move one against the other and eventually would stop each others. A residual trivial motion will be present only in those columns populated by particles moving all in the same direction.

In the following, we study the model for a wide choice of the parameters; the reader should always keep in mind that the values relevant for pedestrian flow scenarios are $r \ll 1$ and $h \gg 0$. Indeed, a walker will change his direction of motion only in the presence of an opposing pedestrian (or other obstacle) and in such a case he will do it almost surely.

The vertical boundaries are considered as occupied sites, that is to say, reflecting boundary conditions are imposed on those vertical boundaries of the strip Λ . On the other hand, the horizontal boundaries are considered filled with empty spots, so that a particle on the first row trying to jump up will exit the system and, similarly, a particle on the L_2 -th row trying to jump down will exit. Particles which did exit the lattice, when selected for a move, will re-enter the strip with the same horizontal coordinate at row one if own color red, and at row L_2 if the particle is blue, provided the target site is empty. We have not considered strictly imposed vertical periodic boundary conditions – the upper and the lower rows of the strip mimick the presence of doors at the end of the corridor (see, also, Appendix A).

2.3. Observables

Quantitative investigations of the model will be performed by means of the following observables. We call *upward current* at time t , the ratio between the total number of blue particles which exited the system through the top boundary and time. Similarly, we call *downward current* at time t , the ratio between the total number of red particles which exited the system through the bottom boundary and time. Note that both these currents are defined as positive numbers. The currents will be used to detect the presence of jamming in the system. More precisely, since the upward and the downward current will be approximatively equal in all the simulations, we will focus on the *average current*, namely, the average between the upward and the downward currents.

Additionally, to give a quantitative estimate of the presence of lanes in the system, we define a suitable order parameter following closely the ideas proposed in [19] and based on developments from [20] done in the framework of colloidal systems.

Fix the time t and consider a particle labelled by $k \in \{1, \dots, N\}$ such that it lies in the lattice at time t . Let $n_{r,k}(t)$ the total number of red particles occupying cells belonging to the same column as the particle k . Furthermore, let $n_{b,k}(t)$ the total number of blue particles

occupying cells belonging to the same column as the particle k . Then set

$$\phi(t) = \frac{1}{n(t)} \sum_{k=1}^{n(t)} \left[\frac{n_{r,k}(t) - n_{b,k}(t)}{n_{r,k}(t) + n_{b,k}(t)} \right]^2. \quad (2.1)$$

Note that in a state in which blue and red particles moved perfectly in separate lanes, the order parameter would be equal to one. For disordered states, we expect $\phi(t)$ to be small, though strictly positive. In the next sections, we shall use the expression *ordered configurations* when referring to configurations in which red and blue particle occupy different columns.

3. Numerical simulations

We simulate the model introduced in Section 2.2 posed on the strip with side lengths $L_1 = 50$ and $L_2 = 100$. We fix a parameter ρ , called *density*, and the total number of particles will then be $N = \rho L_1 L_2$. The numbers of red and blue particles, N_r and N_b , will differ at most by one and will be such that $N_r + N_b = N$. The values of H , h , r , and ρ will be specified both in the forthcoming discussion of the numerical results and in the caption of the figures.

All simulations are run for 8×10^6 time steps: remember that at each time step N particles are randomly selected for motion. The order parameter is computed by averaging its value each 10^2 time steps starting from the thermalization time 10^6 . The currents are computed by applying the definition (given in Section 2.3) at the end of the simulation. The computed observables are very stable and the statistical errors are not significative, hence they are not reported in the pictures.

Aiming to a good vizualization of the effects, the results will be presented by means of two different kind of graphs: configuration pictures and scatter plots. In configuration pictures, each point represents the position of a particle: red points stand for red particles and blue points stand for blue particles. In scatter plots, either the current or the order parameter are reported for approximatively 20×20 different values of the considered parameters evenly spaced in the intervals specified in the graphs. No data interpolation is performed, each measured value corresponds to a square pixel in the picture. The colors shown in scatter plots are adapted to picture data, but in all the pictures blue corresponds to the half of the maximum value in the plot. Moreover, for the values below such half value we use gray tones, whereas for the values above it, we use the following brilliant colors: magenta, red, orange, yellow, and green.

3.1. Preliminary simulations

As we already pointed out in Section 2.3, the order parameter ϕ is a positive number close to one for ordered configurations. On the other hand, it is not clear how small such a parameter will be for disordered configurations. Particularly, we cannot infer that ϕ will be close to zero. Indeed, cf. (2.1), ϕ is defined as a sum of positive numbers, so that fluctuations in random configurations will add up and not cancel. Mainly for this reason, we perform a first study of the system for a wide choice of the parameter r . Obviously, we expect that for an r not small, the system will be essentially disordered. In this way, we will give a quantitative measure of the values that the order parameter ϕ should exhibit for disordered states.

In Figure 2, we plot the average current in a scatter plot as a function of the background noise r and the density ρ for different choices of the horizon depth H and of the lateral move probability h . As expected, the highest values of the average current are found for low values of the background noise. Indeed, as already noted, when r is small, particles experience an important forward drift. Nevertheless, seeing the left diagram in the picture, we realize that when $H = 0$ for some intermediate value of the density (focus, for instance, to the case $\rho = 0.15$), the current, which is negligible for r small, becomes important if r is mildly increased, but it eventually becomes zero for even larger values of the background noise. This effect is due to the fact that, for small values of the background noise, the dynamics is trapped in blocked (clogged) configurations, whereas a larger value of randomness in the dynamics helps particles to avoid blocking opponents restoring the global current to not zero values.

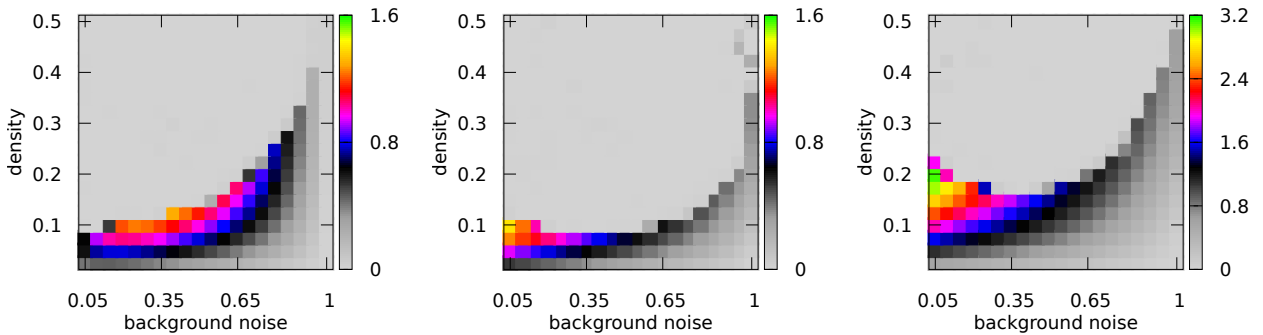


Figure 2: Scatter plot of the average current in the plane r - ρ for $r \in [0.05, 1]$, $\rho \in [0.05, 0.5]$, $H = 0$ (left), $H = 5$ and $h = 0.1$ (center), $H = 5$ and $h = 0.7$ (right).

This is illustrated in Figure 3 where it is reported the final configuration of the system in the simulations for the values of the parameters specified in the caption. The first three panels on the left show that considering larger values of r , in absence of the anticipation

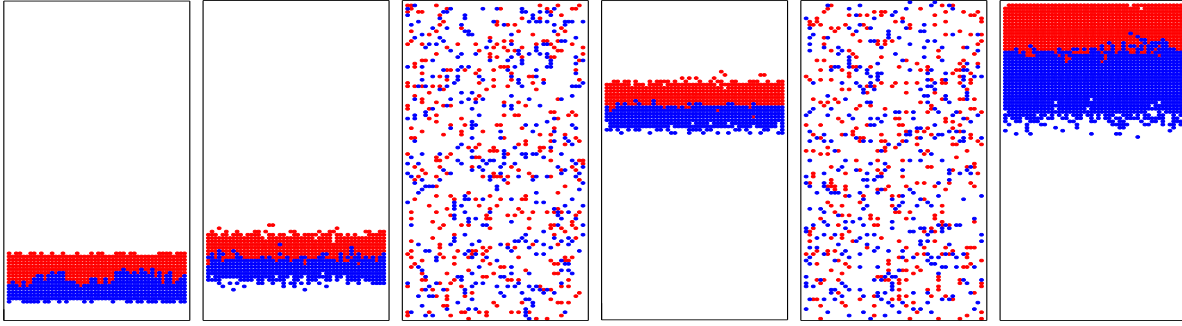


Figure 3: From the left to the right it is depicted the final configuration of the simulations for the cases $H = 0$, $r = 0.1$, and $\rho = 0.15$ (first graph), $H = 0$, $r = 0.5$, and $\rho = 0.15$ (second graph), $H = 0$, $r = 0.7$, and $\rho = 0.15$ (third graph), $H = 5$, $h = 0.1$, $r = 0.5$, and $\rho = 0.15$ (fourth graph), $H = 5$, $h = 0.7$, $r = 0.5$, and $\rho = 0.15$ (fifth graph), and $H = 5$, $h = 0.7$, $r = 0.8$, and $\rho = 0.45$ (sixth graph).

mechanism, allows to avoid blocking configurations. In this respect, randomness favors transport. It is interesting to remark that a similar phenomenon was found by the authors in [5, Figures 6.14 and 6.15], where it was remarked that the so called residence time it is a not monotonic function of the lateral displacement probability. We recall that the residence time was defined in *loc. cit.* as the typical time that a particle started at one side of the strip needs to cross the whole strip and exit from the opposite boundary. Consequently, the residence time and the current are closely related quantities.

Another interesting phenomenon can be observed comparing the second, the fourth and the fifth panels in Figure 3. In these three cases, the values of background noise and density are not changed, but the anticipation effect is introduced and the lateral move probability is changed. The pictures show that adding the anticipation mechanism with a sufficiently large lateral move probability blocking configurations can be avoided. The fact that anticipation helps transport in a wide region of the parameter space is also evident from the current graphs in Figure 2, but the configurations reported in Figure 3 provide a striking evidence. The sixth configuration in Figure 3 shows that for very large values of the density, even a large lateral move probability is not sufficient to the restore current, and consequently, the dynamics is eventually trapped in a blocked configuration.

In Figure 4, we finally come to the main target of this section, namely, the graph of the order parameter in the plane $r-\rho$. The scatter plot is reported for the same cases considered in Figure 2. In all the cases, we do not expect lane formation, due to the rather high values of the background noise considered in the pictures. Indeed, the graphs in Figure 4 show

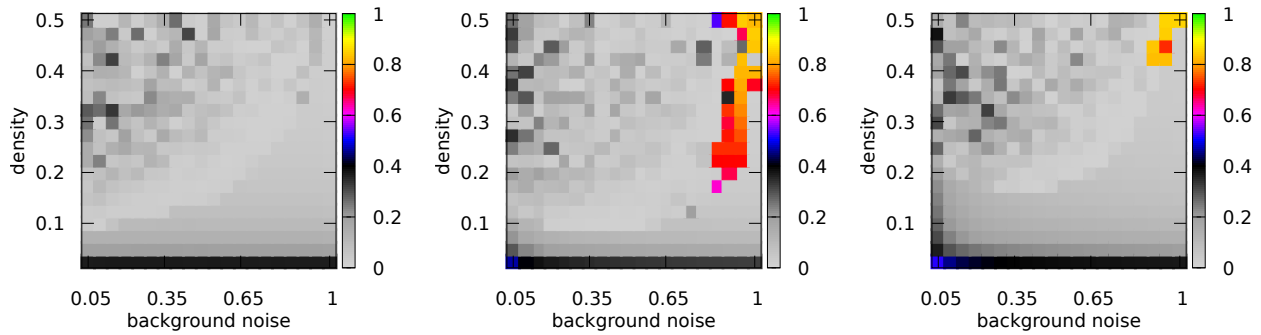


Figure 4: Scatter plot of the order parameter ϕ in the plane r - ρ for the same case considered in Figure 2.

that the order parameter is approximatively constant in the whole region considered in the simulations. Moreover, the stationary value of the order parameter ranges between 0.1 and 0.3. Hence, in the sequel of our discussion we will consider such a value as the reference point of the order parameter for completely disordered configurations. The small islands in the central and right panel corresponding to higher values of the order parameter can be neglected since they are observed in correspondence of blocked configurations. The relative high value of ϕ is just a random value depending on the random initial condition, for instance in the case illustrated in the sixth panel in Figure 3. This is due to the fact that, in the final configuration, many red particles remained blocked outside the lattice, hence in each column a majority of red particles is present. This yields in a rather high value of the order parameter.

3.2. Small background noise

We now focus on the most interesting part of the parameter space, namely, the region with small background noise.

In Figure 5, we have reported the results of our simulations at $r = 0$, namely, when no background noise is present so that the sole mechanism present in the dynamics is anticipation: particles move in their prescribed forward direction unless an opposing particle is spotted inside the horizon region. In the picture, we show scatter plots in the plane h - ρ for both the average current and the order parameter ϕ .

The left panel gives evidence that at any value of the lateral move probability, the average current increases with the density if this is sufficiently small, i.e., smaller than about 0.3. On the other hand, when such a value is reached, the dynamics freezes in blocked configurations, and hence, the currents suddenly drop to zero. It is quite remarkable that *the current, when different from zero, does not depend very much on the lateral move probability h* . On the

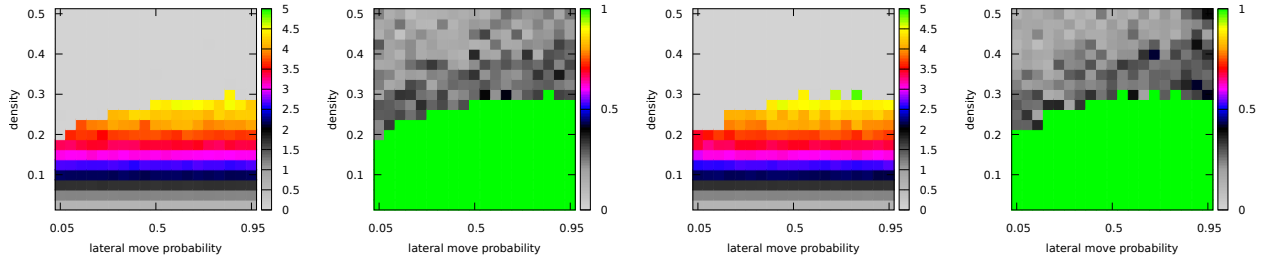


Figure 5: Scatter plot of the current (first and third panel) and order parameter ϕ (second and fourth panel) in the plane h - ρ for zero background noise, $h \in [0.05, 0.95]$, $\rho \in [0.05, 0.5]$, $H = 5$ (first two panels), and $H = 20$ (third and fourth panel).

other hand, as we have already noted in the above Section 3.1, for intermediate values of the density the anticipation mechanism helps transport, in the sense that the freezing of the dynamics occurs at larger value of the density if h is large.

To emphasize this point aspect in a better way, we have plotted in Figure 6 the final simulation configuration of the system at density $\rho = 0.275$, for different values of the lateral move probability h . The pictures shows that if h is small the dynamics is eventually trapped in a blocked configuration whereas as h is increased no freezing is observed, at least on the time scale we considered, and the current results to be different from zero.

We finally remark that, for $r = 0$, if the dynamics is not trapped then the order is perfect, namely, $\phi = 1$ is reached. In other words, *in the absence of the background noise, the anticipation mechanism guarantees a perfect lane formation, provided the dynamics is not frozen in blocked configurations*. In our opinion, this is a very valuable result, since it states that lanes forming in counterflows can be explained just as a consequence of the anticipation mechanism.

Data referring to the case $H = 20$ and reported in Figures 5 and 6 can be discussed similarly; the only difference is that the effect of the anticipation mechanism is slightly stronger. This fact can be observed both in Figure 5 and 6.

We test if the anticipation mechanism is robust with respect to the background noise, that is to say, if its ability to form lanes is still valid for r different from zero.

In Figures 7 and 8 we report the scatter plot of the average current and the order parameter on the r - ρ plane for different values of the lateral move probability. In particular, the left panel refers to the case in which the anticipation mechanism is not present in the dynamics.

We pinpoint here a behavior which is very similar to the one discussed in the case $r = 0$. In particular, we notice that, for a fixed value of the density ρ , increasing the lateral move

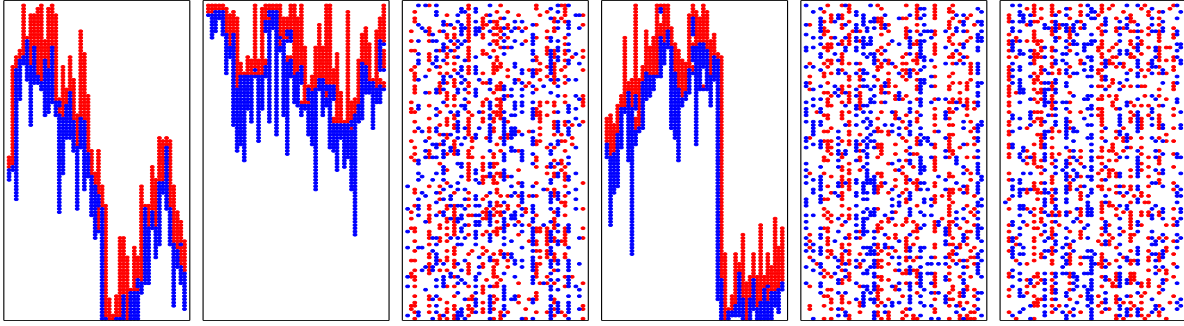


Figure 6: From the left to the right it is depicted the final configuration of the simulations for the cases $r = 0$, $\rho = 0.275$, $H = 5$ and $h = 0.05$ (first graph), $H = 5$, and $h = 0.45$ (second graph), $H = 5$, and $h = 0.50$ (third graph), $H = 20$ and $h = 0.05$ (fourth graph), $H = 20$ and $h = 0.45$ (fifth graph), and $H = 20$ and $h = 0.50$ (sixth graph).

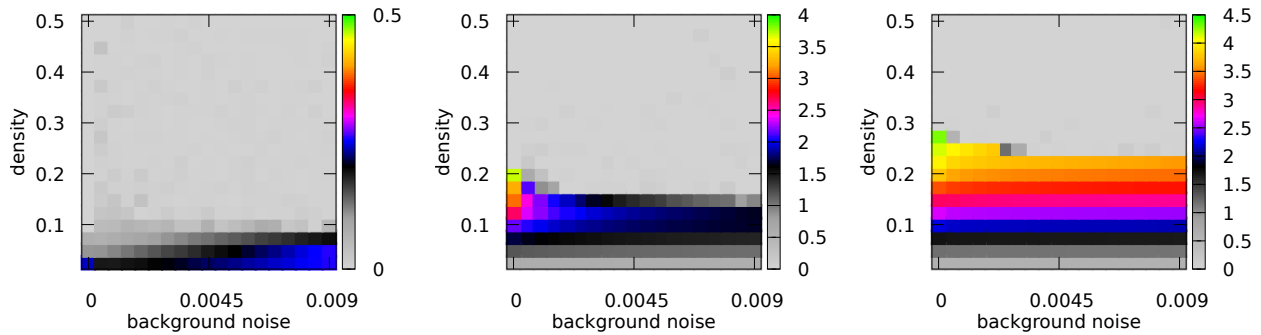


Figure 7: Scatter plot of the average current in the plane r - ρ for $r \in [0, 0.09]$, $\rho \in [0.05, 0.5]$, $H = 0$ (left), $H = 5$ and $h = 0.11$ (center), $H = 5$ and $h = 0.71$ (right).

probability avoids the freezing of the dynamics at larger values of the density ρ . Note also, that the current does not depend very much on the value of the disorder parameter in the considered range. This is quite obvious since in these pictures we are focussing on a very tiny slice of the part of the graphs shown in Figures 2 and 4, very close to the vertical axis.

Finally, we remark that Figure 8 shows that the anticipation mechanism is able to explain lane formation also in the presence of a weak background noise. Such an order is eventually destroyed if the parameter r becomes too large as underlined by the data reported in Figure 4.

4. Discussion

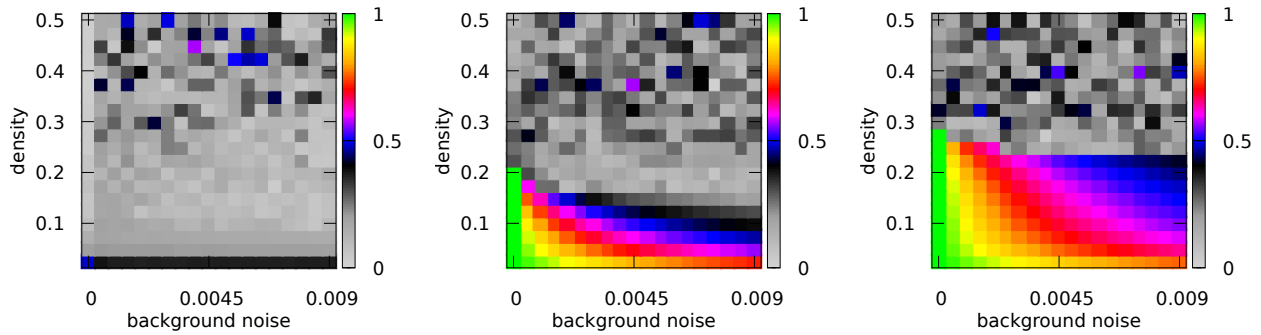


Figure 8: Scatter plot of the order parameter ϕ in the plane r - ρ for the same case considered in Figure 7.

As closing note, in the same line of thinking as in Ref. [24], we argue that the key towards an even deeper understanding of a collective behavior like lane formation lies in identifying the principles of the behavioral algorithms followed by each individual, and also, in answering the question: How does information flow among the pedestrians? Addressing this question requires the embedding in our model of fine environmental psychology information as well as aspects of the psychology of groups. We have not touched these aspects at all in this contribution. This can be seen as further work. On the hand, for the presented bi-directional pedestrian flow scenario, given two population sizes walking within the strip Λ , we are convinced that the simple combination of just 3 parameters is sufficient to predict the formation of lanes. These parameters are the horizon depth H , the lateral move probability h , and the background noise r . This level of complexity is much lower than what usually the social force model is offering. Furthermore, our three parameters have a clear physical meaning. The harder to identify is eventually the background noise level r , which on top of everything is also prone to different modeling interpretations and incorporates very much the specifics of the local conditions (geometry of the building, local traffic, etc.).

Two main results stand out:

- (A) In the absence of the background noise, the anticipation mechanism guarantees a perfect lane formation, provided the dynamics is not frozen in blocked configurations;
- (B) The current does not depend very much on the lateral move probability h .

An interesting question is to which extent (A) and (B) hold if pedestrians would be moving at different speeds? This question, connecting pedestrian flow to traffic flow matters, could be addressed rather naturally using a continuous time version of the present model

in which pedestrian moving at different speeds would be modelled by particles moving with different rates.

Acknowledgements

We thank Prof. Rutger van Santen (Eindhoven, NL) for very fruitful discussions on closely related matters. ENMC thanks the ÉNS de Paris for the very kind hospitality in the period in which part of this work has been done.

A. Strict periodic boundary conditions

As we have already mentioned in the above discussion, we considered "not strictly imposed vertical periodic boundary conditions". Our choice is motivated by the fact that the upper and the lower boundaries are thought as two open doors for the pedestrian motion. In this appendix, we show some minimal results obtained in the case when vertical periodic boundary conditions are strictly imposed as it is usually the case in the statistical mechanics of lattice models. By "strictly imposed" we simply mean that the updating rule is covariant in the lattice and the rows 0 and $L_2 + 1$ are respectively identified with the rows L_2 and 1.

We have repeated the simulations shown in the first two panels of Figure 5 and in the third panel of Figures 7 and 8. Our results, now plotted in Figure 9, do not show new features with respect to what has been discussed above.

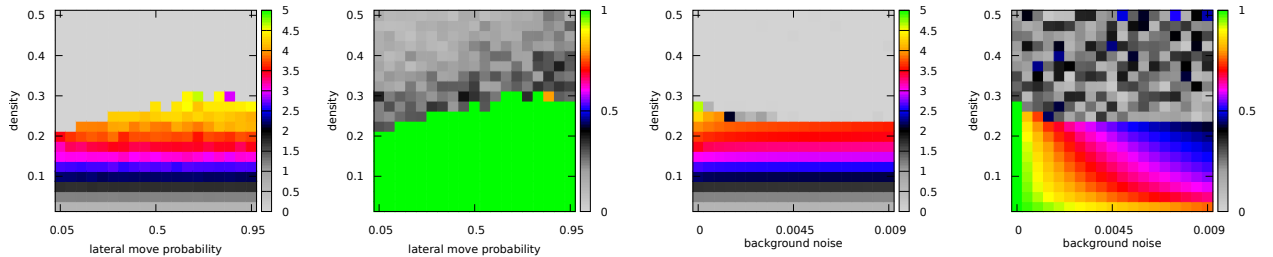


Figure 9: Scatter plot of the current (first and third panel) and order parameter ϕ (second and fourth panel) for the strict periodic dynamics. In the first two panels $H = 5$ and $r = 0$. In the third and fourth panels $H = 5$ and $h = 0.71$.

References

- [1] C. Appert-Rolland, P. Degond, S. Motsch, Two-way multi-lane traffic model for pedestrians in corridors. *Netw. Heterog. Media*, **6** 351-381, (2011).
- [2] R. Bailo, J. A. Carrillo, P. Degond, Pedestrian models based on rational behaviour. *arXiv* 1808.07426, May 2019.
- [3] N. Bellomo, C. Dogbé. On the modeling of traffic and crowds: A survey of models, speculations, and perspectives. *SIAM Review* **53**(3), 409–463 (2011).
- [4] C. Burstedde, K. Klauck, A. Schadschneider, J. Zittartz, Simulation of pedestrian dynamics using a 2–dimensional cellular automaton. *Physica A* **295**, 507–525 (2001).
- [5] E.N.M. Cirillo, O. Krehel, A. Muntean, R. van Santen, A. Sengar, Residence time estimates for asymmetric simple exclusion dynamics on strips. *Physica A* **442**, 436–457 (2015).
- [6] E.N.M. Cirillo, O. Krehel, A. Muntean, R. van Santen, A lattice model of reduced jamming by barrier. *Physical Review E* **94**, 042115, (2016).
- [7] E.N.M. Cirillo, A. Muntean, Can cooperation slow down emergency evacuations? *Comptes Rendus Mécanique* **340**, 6260–628 (2012).
- [8] E.N.M. Cirillo, A. Muntean, Dynamics of pedestrians in regions with no visibility – a lattice model without exclusion. *Physica A* **392**, 3578–3588 (2013).
- [9] P. Degond, J. Hua, Self-organized hydrodynamics with congestion and path formation in crowds. *J. Comput. Phys.* **237** 299-319 (2013).
- [10] M. Doi, *Soft Matter Physics*, Oxford University Press, 2013.
- [11] J.H.M. Evers A. Muntean, Modeling micro-macro pedestrian counter flow in heterogeneous domains. *Nonlinear Phenomena in Complex Systems* **14**, 1, 2737 (2011).
- [12] P. Gerlee, K. Tunstrom, T. Lundh, B. Wennberg, Impact of anticipation in dynamical systems, *Phys. Rev. E* **96**, 062413 (2017).
- [13] D. Helbing, A mathematical model for the behavior of pedestrians. *Behavioral Science* **36**, 298–310 (1991).

- [14] D. Helbing, I.J. Farkas, P. Molnár, T. Vicsek, Simulation of pedestrian crowds in normal and evacuation situations. In *Pedestrian and Evacuation Dynamics* (2002), pp. 21-58, edited by M. Schreckenberg and S.D. Sharma.
- [15] D. Helbing, T. Platkowski, Self-organization in space and induced by fluctuations. *International Journal of Chaos Theory and Applications* **5**, 25–39 (2000).
- [16] D. Helbing, T. Vicsek, Optimal self-organization. *New Journal of Physics* **1**, 13.1–13.17 (1999).
- [17] S. Heliövaara, T. Korhonen, S. Hostikka, H. Ehtamo, Counterflow model for agent-based simulation of crowd dynamics, *Building and Environment* **48**, 89–100 (2012).
- [18] H. Murakami, C. Feliciani, K. Nishinari, Lévy walk process in self-organization of pedestrian crowds. *J. R. Soc. Interface*, **16**, 20180939 (2019).
- [19] S. Nowak, A. Schadschneider, Quantitative analysis of pedestrian counterflow in a cellular automaton model. *Phys. Rev. E* **85**, 066128 (2012).
- [20] M. Rex, H. Löwen, Lane formation in oppositely charged colloids driven by an electric field: chaining and two-dimensional crystalization *Physical Review E* **75**, 051402 (2007).
- [21] I. Serrano, B. Suceava, A. Verdugo, Pleasure, imagination, fear and joy: applied themes in Nicole Oresmes De Configurationibus. *Memoirs of the Scientific Sections of the Romanian Academy*, **XLI**, 7–20 (2018).
- [22] T. Shimaya, K. A. Takeuchi, Lane formation and critical coarsening in a model of bacterial competition. *Phys. Rev. E*, **99**, 4, 042403 (2019).
- [23] Y. Suma, D. Yanagisawa, K. Nishinari, Anticipation effect in pedestrian dynamics: modeling and experiments. *Physica A* **391**, 248–263 (2012).
- [24] D.J. Sumpter, The principles of collective animal behaviour. *Philos Trans R Soc Lond B Biol Sci.* **361**, 1465, 5–22 (2006).